IJNRD.ORG ISSN : 2456-4184
INTERNATIONAL JOURNAL OF NOVEL RESEARCH AND DEVELOPMENT (IJNRD) | IJNRD.ORG
An International Open Access, Peer-reviewed, Refereed Journal

EFFECT OF JOULE HEATING ON THERMALLY RADIATING HYDROMAGNETIC CONVECTIVE SQUEEZING THREE-DIMENSIONAL FLOW OF WATER ETHYLENE GLYCOL BASED TITANIA (TiO_2) NANOFLUID IN A VERTICAL CHANNEL

[1]B. Sreenivasa Reddy and [2]A.Malleswari
[1]Associate Professor, [2]Research Scholar
[1&2]Department of Applied Mathematics, Yogivemana University, Kadapa, A.P., India,

Abstract : The main objective of the present investigation is to study Hall current effects on the three dimensional squeezing flow of TiO_2 nanofluid with water and Ethylene Glycol(Eg) base fluids in a vertical channel and its heat transfer characteristics. The governing equations are reduced to set of ordinary differential equations and then numerically solved by employing Runge-Kutta-Fehlberg fourth-fifth order method. Effect of pertinent parameters on velocity, temperature fields is examined through the plots. Skin-friction coefficients, Nusselt number for different variations are studied numerically. The authors have hope that the results obtained in the present study not only provide useful information for applications, it also serves as a complement to the previous studies.

1.INTRODUCTION:

Dissipation is the strait of metamorphosing mechanical energy of downward-flowing water into acoustical and thermal energy. Viscous dissipation effects play a momentous role in free convection in various devices which are operated at high speeds. To define the viscosity of dilute suspensions, dissipation function is used (Einstein [39]). Viscous dissipation with magneto hydrodynamic flow has many momentous geothermal, technological and industrial applications such as MHD accelerators and MHD power generation, liquid, and metal nuclear reactors. When the flow field is in high gravitational field or at low temperature or of exhaustive size, the viscous dissipation heat in the free convective flow is momentous. The importance of viscous dissipative heat in free convection flow in the case of constant heat flux and isothermal at the plate has been demonstrated and implicit finite difference method of Crank-Nicolson's type to obtain the numerical solution heat transfer on MHD through electrical conductivity by Gebharat [40], Kishore et al. [41], Sakiadis [42], Jewel Rana et al.[43].

After the outstanding development of nanotechnologies in early 1990, a new type of suspension containing nanoparticles called nanofluid has appeared. These nanofluids have gained attention due to their importance in improving the efficiency of thermal systems. The nanoparticles may be metals, oxides, carbides or nitrites, while the base fluid may be water, kerosene, motor oil, tolune, ethylene and tri-ethylene glycol are according to the process used.

However, the heat transfer efficiency also depends on the thermal performance of working fluids. Thus, improving the thermal conductivity of working fluids becomes a major and challenging task for industrial necessity. The inspiration of suspended nanoparticles in a base fluid to increase the thermal conductivity was proposed by Choi [5] about a decade ago. Thereafter, theoretical and experimental investigations on the nanofluid heat transfer property have been conducted by Wang et al. [37], Eastman et al. [10], Buongiorno [3], etc. They have concluded that the thermal conductivity of the base fluid can be dramatically enhanced in the presence of nanoparticles. Besides, there are two models are available to incorporate nanoparticle effect on fluid flow problems namely single phase model and two-phase model. Further, Buongiorno or Tiwari and Das model is used to model the single-phase nanofluid.

It has been established by Chen et al [4] on measuring the effective thermal conductivity that improvement in Tio2 nanoparticles and Tio2 nanotubes with Ethylene glycol as base fluids are higher than those with water as a base fluid. Several authors have (Das [6], Hamad and Pop [13], Sheikholeslami and Ganji [30, 31], Turkyilmazoglu, Turkyilmazoglu & Pop [34, 35]) studied the MHD effects on nanofluid flow in a permeable channel. Kuznetsov and Nield [18] critically analyzed the natural

convection flow of a nanofluid past a vertical plate. A comparison of MHD convective flow Tio2 –water and Al2o3-water nanofluids is made by Reddy and Chamkha [28]. Mebarek-Oudina [21, 22] numerically investigated convective heat transfer of nanofluids in an annular space between two vertical coaxial cylinders containing a constant heat source. Pak and Cho [27] experimentally analysed improvements in heat transfer with Tio2 and Al2o3 nanofluids in a pipe under turbulent flow condition and suggested Nusselt number correlation.

In this study, Tio2 nanofluids are used, where they appear in various applications particularly in energy systems. With the development of hat transfer process, the sector of application of Tio2 nanofluids expands in the fields of solar collectors, heat pipes, energy storage refrigeration, and other energy applications. The thermal conductivity of the Tio2 nanofluids can be affected by the ingredients of the base fluids.

On the other hand, an unsteady squeezing flow of an electrically conducting fluid occurs in many engineering and industrial applications such as lubrication, food industries, transient loading of mechanical components, power transmission, polymer processing, compression and injection modelling. The squeezing flow of a fluid was first introducing by Stefan [33], Following this work, many researchers have investigated such flow with different aspects. Numerical solution for a fluid film squeezed between two parallel plane surfaces have been reported by Hamza and Macdonald [15], Domairry and Aziz [9], Mustafa et al [24], Hamza [14], Munawar et al [23], Hayat et al [16], Mahantesh et al[19], Freidoonimehr et al. [11], Gireesha et al. [12], Das [6].

To accurately predict the flow the heat transfer rate, it is necessary to take into account this cariation of viscosity. Convection flow in nature and engineering phenomena requires that viscosity and thermal conductivity of fluids vary with temperature. For instant, the viscosity for dry air at 100^0 C is 21.94x10-56 kg/ms while at 200^0 C it is $26.94x10^{-6}$ kg/ms, Ali [1] was briefly discussed the effect of variable viscosity on mixed convection heat transfer along a vertical moving surface. Vajravelu et al [36], and Issac and Anselm [17] showed that, velocity distribution decreases with increase in viscosity while the temperature profiles increase with increase in variable viscosity. Several authors [Devi and Prakash [8], Sreenivasulu et al[32], Makinde[20], Satya Narayana and Ramakrishna [29], Nagasasikala [25], Devasena[7]) one step used to variable viscosity of the MHD flow of a variable viscosity nanofluid over a radially stretching convective surface with radiative heat.

Recently Tulasilakshmidevi and Sreenivasa Reddy [38] have brief discussed about three-dimentional squeezing flow of Ttania nanofluid in different base fluids with heat sources and this research work was comparison with their results.

In this research paper, authors have been discussed the heat transfer characteristics of Hall current effects on the three dimensional squeezing flow of TiO_2 nanofluid with water and Ethylene Glycol(Eg) base fluids in a vertical channel. For different parametric variables and tabular values on velocity, temperature fields are examined through the plots. Skin-friction coefficients, Nusselt number for different variations are studied numerically. The authors have hope that the results obtained in the present study not only provide useful information for applications, it also serves as a complement to the previous studies.

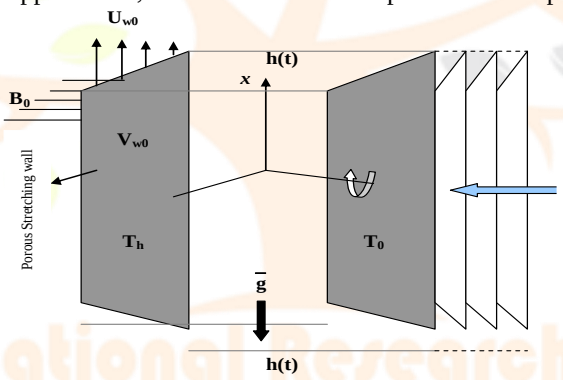

Figure 1 : Flow configuration and coordinate

2. MATHEMATICAL FORMULATION

Consider an unsteady three-dimensional squeezing flow of Tio2 nanofluid with water and Ethylene Glycol base fluids in a vertical channel. The plane positioned at $y = 0$ is stretched with velocity $U_{wo} = ax/(1 - \alpha t)$ in x-direction and maintained at the constant temperature T_0 and concentration Co. The temperature at the other plane is T_h and located at a variable distance $h(t) = \sqrt{\nu_f (1-\alpha t)}$. In negative y-direction, the fluid is squeezed with a time dependent velocity $V_h = dh/dt = -\alpha/2\sqrt{\nu_f/\alpha(1-\alpha t)}$. The fluid and the channel are rotated about y-axis with angular velocity $\vec{\Omega} = \omega\hat{j}/(1-\alpha t)$. The transverse magnetic field is assumed to be variable kind $\vec{B} = B_0/\sqrt{(1-\alpha t)}$ and it is applied along y-axis. The fluid is sucked/injected from the plane located at $y = 0$ as shown in figure 1. The magnetic Reynolds number is assumed to be small thus induced magnetic field is negligible. In addition, effects of Hall current, viscous dissipation and Joule heating are neglected.

Under those assumptions, the governing equations with Hall effects and non-linear thermal radiation for the velocity and temperature fields in the presence of internal heating source are given by [*Hayat et al* 2015 [16], *Munawar et al* 2012 [23]].

$$\frac{\partial u}{\partial x} + \frac{\partial v}{\partial y} = 0, \tag{2.1}$$

$$\frac{\partial u}{\partial t} + u\frac{\partial u}{\partial x} + v\frac{\partial u}{\partial y} = -\frac{1}{\rho_{nf}}\frac{\partial p}{\partial x} + \frac{1}{\rho_{nf}(1-\phi)^{2.5}}\left[\frac{\partial}{\partial x}\left(\mu_f\left(\frac{\partial u}{\partial x}\right)\right) + \frac{\partial}{\partial y}\left(\mu_f\left(\frac{\partial u}{\partial y}\right)\right)\right] - (u + mw) + \frac{g(\rho\beta_T)_{nf}}{\rho_{nf}}(T - T_0), \tag{2.2}$$

$$\frac{\partial v}{\partial t} + u\frac{\partial v}{\partial x} + v\frac{\partial v}{\partial y} = -\frac{1}{\rho nf}\frac{\partial p}{\partial y} + \frac{1}{\rho_{nf}(1-\phi)^{2.5}}\left[\frac{\partial}{\partial x}\left(\mu_f\left(\frac{\partial v}{\partial x}\right)\right) + \frac{\partial}{\partial y}\left(\mu_f\left(\frac{\partial v}{\partial y}\right)\right)\right], \tag{2.3}$$

$$\frac{\partial w}{\partial t}+u\frac{\partial w}{\partial x}+v\frac{\partial w}{\partial y}=\frac{1}{\rho_{nf}(1-\phi)^{2.5}}[\frac{\partial}{\partial x}(\mu_f(\frac{\partial w}{\partial x})+\frac{\partial}{\partial y}(\mu_f(\frac{\partial w}{\partial y})]+\frac{\sigma B_0^2}{\rho nf\,(1-\alpha t)}(mu-w), \quad (2.4)$$

$$\frac{\partial T}{\partial t}+u\frac{\partial T}{\partial x}+v\frac{\partial T}{\partial y}=\frac{k_{nf}}{(\rho C_p)_{nf}}\left(\frac{\partial^2 T}{\partial x^2}+\frac{\partial^2 T}{\partial y^2}\right)+\frac{Q_0}{(\rho C_p)_{nf}(1-\alpha t)}(T-T_0)-$$
$$-\frac{1}{(\rho C_p)_{nf}}\frac{\partial(q_R)}{\partial y}+\frac{2\mu_{nf}}{(\rho C_p)_{nf}}[(\frac{\partial u}{\partial y})^2+(\frac{\partial v}{\partial y})^2]+\frac{\sigma_{nf}\mu_e^2 H_o^2}{(\rho C_p)_{nf}}(u^2+v^2) \quad (2.5)$$

where u, v and w are velocity components along x,y and z directions respectively, p is pressure. B_0 is the magnetic field, σ is the electrical conductivity, g is the magnitude of acceleration due to gravity, α is characteristic parameter with the dimension of reciprocal of time t and $\alpha t < 1$. T is temperature of the fluid Q_0 is uniform volumetric heat generation/ absorption; here $Q_0<0$ and $Q_0 > 0$ are respectively corresponds to internal heat absorption and generation, ρ_{nf} is effective density of the nanofluid, $\nu_{nf} = \mu_{nf} / \rho_{nf}$ is effective kinematic viscosity of the nanofluid, k_{nf} and $(\rho C_p)_{nf}$ are effective thermal conductivity and heat capacity of the nanofluid respectively. They are defined as follows;

$$\rho_{nf}=(1-\varphi)\rho_f+\varphi\rho_s,\ (\rho\beta)_{nf}=(\varphi)(\varphi\beta)_f+\varphi(\rho\beta)_s,\ (\rho C_p)_{nf}=(1-\varphi)(\rho C_p)_f+\varphi(\rho C_p)_s$$
$$\mu_{nf}=\frac{\mu_f}{(1-\varphi)^{2,5}},\ \frac{k_{nf}}{k_f}=\frac{(k_s+2k_f)-2\varphi(k_f-k_s)}{(k_s+2k_f)+2\varphi(k_f-k_s)} \quad (2.6)$$

where the subscripts *nf*, *f* and *s* represent the thermo physical properties of the nanofluid, base fluid and the nanosolid particles respectively and ϕ is the solid volume fraction of the nanoparticles. The thermo physical properties of the nanofluid are given in

The thermo physical properties of the nanofluids are given in Table 1 (See ***Oztop and Abu-Nada*** (2008).

Table – 1 : Physical Properties of nanofluids

Physical properties	Fluid phase (Water)	Fluid phase (Ethylene Glycol)	Tio2 nanofluid
C_p(j/kg K)	997.1	1115	686.2
ρ(kg m^3)	4179	2430	4250
k(W/m K)	0.613	0.253	9.9538
βx10^{-5} 1/k)	21	5.7	0.90
σ	**5.5x10^{-6}**	**10.7x10^{-5}**	6.27x10^{-5}

The approximate boundary conditions for the present problem are;

$$\left.\begin{aligned} &u(x,y,t)=U_{w0}, \quad v(x,y,t)=V_{w0}, \\ &w(x,y,t)=0, \quad T(x,y,t)=T_0, \end{aligned}\right\} \text{ at } y=0 \quad (2.7)$$

$$\left.\begin{aligned} &u(x,y,t)=0, \quad v(x,y,t)=V_h, \\ &w(x,y,t)=0, \quad T(x,y,t)=T_h, \end{aligned}\right\} \text{ at } y=h(t) \quad (2.8)$$

where $T_h=T_0+T_0/(1-\alpha t),, V_{w0}=-V_0/(1-\alpha t)$. Here V_0 is constant, $V_{w0} < 0$ corresponds injection whereas $V_{w0} > 0$ corresponds wall suction.

The dynamic viscosity of the nanofluids is assumed to be temperature dependent as follows:

$$\mu_f(T)=\mu_0 Exp(-m(T-T_1)) \quad (2.9)$$

where μ_{nf} is the nanofluid viscosity at the ambient temperature To, m is the viscosity variation parameter which depends on the particular fluid.

The radiation heat term(***Brewster***[2]) by using The Rosseland approximation is given by

$$q_r=-\frac{4\sigma^{\bullet}}{3\beta_R}\frac{\partial T'^4}{\partial y} \quad (2.10)$$

$$T'^4\cong 4TT_0^3-3T_0^4 \quad (2.11)$$

where $\sigma^{\bullet}$ is the Stefan –Boltzman constant and β_R is the mean absorption constant.

The non-dimensional temperature $\theta(\eta)=\frac{T-T_h}{T_o-T_h}$ can be simplified as

$$T=T_0(1+(\theta_w-1)\theta) \quad (2.12)$$

where $\theta=\frac{T_0}{T_h}$ is the temperature parameter.

To reduce the governing equations into a set of similarity equations, introduce the following similarity transformations [***Munawar et al*** 2012[23]].

$$\psi = \sqrt{\frac{\alpha \nu_f}{1-\alpha t}} x f(\eta),\ \eta = \frac{y}{h(t)}, T = T_0 + \frac{T_0}{1-\alpha t}\theta(\eta),$$

$$u = U_{w0} f_\eta \eta, \qquad v = -\sqrt{\frac{\alpha \nu_f}{1-\alpha t}} f(\eta), \qquad w = U_{w0} g(\eta), \tag{2.13}$$

where a suffix η denote the differentiation with respect to η and ν_f is the kinematic viscosity of the base fluid. Using the above transformations (2.13), the equation (2.1) is automatically satisfied, while the equation (2.2) – (2.5) are respectively reduces to the following nonlinear ordinary differential equations;

$$f_{\eta\eta\eta} - B f_{\eta\eta}\theta_\eta = Exp(\mathrm{B}\theta)\left[f\, f_{\eta\eta} - f_\eta^2 - \beta\left(f_\eta \frac{\eta}{2} f_{\eta\eta}\right) - \frac{\rho_f}{\rho_{\eta f}} M^2 f_\eta + \frac{(\rho\beta)_{\eta f}}{\rho_{\eta f}} Gr_m \theta \right] \tag{2.14}$$

$$= \frac{(1-\alpha t)^2 (1-\phi)^{2.5} e^{B\theta}}{a^2 x} \frac{\partial p}{\partial x},$$

$$f_{\eta\eta} - B f_\eta \theta_\eta + Exp(B\theta)\left[-f\, f_\eta + \frac{\beta}{2}\left(f + \eta f_\eta \right)\right] = -\frac{(1-\alpha t)(1-\phi)^{2.5} e^{B\theta}}{\mu_0 a} p_\eta, \tag{2.15}$$

$$g_{\eta\eta} - B g_\eta \theta_\eta + Exp(B\theta)\left(\left[f\, g_\eta - f_\eta g - \beta\left(g\ \frac{\eta}{2} g_\eta \right)\right] - \frac{\rho_f}{\rho_{\eta f}} M^2 g\right) = 0, \tag{2.16}$$

$$Rd[(1+(\theta_w - 1)\theta^3)\theta']' + {}^2 \frac{k_f}{k_{nf}} \Pr\left[A_3 \left\{ \beta\left(\theta + \frac{\eta}{2}\theta_\eta \right) + f\theta_\eta \right\} + Q\theta \right].$$

$$+ \frac{k_f}{k_{nf}} [2Ec \Pr\{(\frac{\partial^2 f}{\partial y})^2 + (\frac{\partial g}{\partial y})^2\} + \mathrm{M}^2 \mathrm{Ec} \Pr A_6\{(\mathrm{f}')^2 + g^2\}] = 0 \tag{2.17}$$

The transformed boundary conditions are;

$f_\eta = 1,\quad f = \mathrm{fw},\quad g = 0,\quad \theta = 0,\quad$ at $\quad \eta = 0$

$f_\eta = 0,\quad f = \frac{\beta}{2},\quad g = 0,\quad \theta = 1\ ,\quad$ at $\quad \eta = 1$ (2.18)

where

$\beta = (\alpha/a)$ is the squeezing parameter, $B = m(T_0 - T_1)$ is the viscosity parameter, m = $(\omega_e \tau_e)$ is Hall parameter, $M^2 = \sigma B_0^2 / \alpha \rho_f$ is magnetic parameter, $Gr_m = Gr / Re^2$ is mixed convection parameter, $Gr = g(\beta_T)_f T_0 x^3 / \nu_f^2 (1-\alpha t)$ is modified Grashaf number, $Re = xU_{w0} / \nu_f$ is Reynolds number, $Pr = (\mu c_p)_f / k_f$ is the Prandtl number, $Q = Q_0 / \alpha(\rho C_p)_f$ is heat source / sink parameter and $fw = V_{w0} / \alpha h$ is suction / injection parameter. $Q = Q_0 / \alpha(\rho C_p)_f$ is heat source / sink parameter, $Rd = \frac{4\sigma^* T_o^3}{k_f \beta_R}$ is the Radiation parameter, $Ec = \frac{U_{wo}^2}{(\rho C_p)_f T_0}$ is the Eckert number(verify), $\theta_w = \frac{T_w}{T_0} = A$ is the temperature difference ratio, $A_1 = \frac{1}{(1-\varphi)^{2.5}}, A_2 = (1-\varphi) + \varphi(\frac{\rho_s}{\rho_f}), A_3 = 1 - \varphi + \varphi\frac{(\rho C_p)_s}{(\rho C_p)_f}, \ A_4 = 1 - \varphi + \varphi(\frac{(\rho\beta)_s}{(\rho\beta)_f}, \ A_5 = \frac{k_{nf}}{k_f} \ \ A_6 = (1 + \frac{3(1-\sigma)\phi}{(\sigma+2)}), \sigma = \frac{\sigma_s}{\sigma_f}$

It is important to mention that, β = 0 represents plates are stationary, β > 0 corresponds to the plate which is located at $y = h(t)$ moves towards the plate which is located at $y = 0$ and β <0 corresponds to the plate at $y = y(t)$ moves apart with respect to the plate at $y = 0$.

For engineering and industrial point of view, one has usually less interest in velocity and temperature profiles nature than in the value of the skin-friction and rate of heat transfer. Therefore expression for the local skin-friction coefficient and the local Nusselt number at both the walls are defined as;

$$C^*_{f,\ \text{at } y=0} = \frac{(\tau_{xy})_{y=0}}{\rho_{\eta f} U_{w0}^2}, \qquad C^*_{f,\ \text{at } y=h(t)} = \frac{(\tau_{xy})_{y=h(t)}}{\rho_{\eta f} U_{w0}^2}, \tag{2.19}$$

$$Nu^*_{\ \text{at } y=0} = \sqrt{\frac{\nu_f}{a}} \frac{(q_{xy})_{y=0}}{k_f T_0}, \qquad Nu^*_{\ \text{at } y=h(t)} = \sqrt{\frac{\nu_f}{a}} \frac{(q_{xy})_{y=h(t)}}{k_f T_0}, \tag{2.20}$$

where τ_{xy} is the shear stress and q_{xy} is the heat flux, which are given by

$$\tau_{xt} = \mu_{\eta f}\left(\frac{\partial u}{\partial x} + \frac{\partial u}{\partial y} \right) \quad \text{and} \quad q_{xt} = -k_{\eta f}\left(\frac{\partial T}{\partial x} + \frac{\partial T}{\partial y} \right) \tag{2.21}$$

In view of equation (2.20) and similarity transformations (2.13); equations (2.19)-(2.20) will takes the following form;

$$C^*_{f,\ \text{at } y=0} = \sqrt{\mathrm{Re}}\, C^*_{f,\ \text{at } y=0} = f_{\eta\eta}(0)/(1-\phi)^{2,5}\left(1 - \phi + \phi\left(\frac{\rho_s}{\rho_f} \right)\right),$$

$$C^*_{f,\ \text{at } y=h(t)} = \sqrt{\mathrm{Re}}\, C^*_{f,\ \text{at } y=h(t)} = f_{\eta\eta}(1)/(1-\phi)^{2,5}\left(1 - \phi + \phi\left(\frac{\rho_s}{\rho_f} \right)\right),$$

$$Nu_{\text{ at } y=0} = (1-\alpha t)^{1.5}\ Nu^{*}_{\text{ at } y=0} = -\frac{k_{\eta f}}{k_f}\theta_\eta(0),\ Nu_{\text{ at } y=h(t)} = (1-\alpha t)^{1.5}\ Nu^{*}_{\text{ at } y=h(t)} = -\frac{k_{\eta f}}{k_f}\theta_\eta(1) \quad (2.22)$$

3. NUMERICAL METHOD AND VALIDATION

A set of non-similar equations (2.15)-(2.17) are nonlinear in nature and possess no analytical solution, thus, a numerical treatment would be more appropriate. These set of ordinary differential equations together with the boundary conditions (2.14) are numerically solved by employing fourth-fifth order Runge-Kutta-Fehlberg scheme with the help of Maple. This algorithm in Maple is proven to be precise and accurate and which has been successfully used to solve a wide range of nonlinear problem in transport phenomena especially for flow and heat transfer problems. In this study, we set the relative error tolerance to 10^{-6}. Comparison results are recorded in table 1 and are found to be in excellent agreement. The effects of development of the squeezing three-dimensional flow and heat transfer in a rotating channel utilizing nanofluid are studied for different values of squeezing parameter, rotation parameter, magnetic parameter, suction/injection parameter, mixed convection parameter, nanoparticle volume fraction parameter, Prandtl number, radiation parameter and heat source/sink parameter. In the following section, the results are discussed in detail with the aid of plotted graphs and tables.

4.COMPARISION:

Table 3a :In the absence of Eckert number(Ec=0) the results are in good agreement with those of ***Reddy et al*** [38]

Parameter		Water-TiO2 nanofluid Sreenivasa Reddy et al[38]			Water-TiO2 nanofluid Present Results		
		τx(0)	τy(0)	Nu(0)	τx(0)	τy(0)	Nu(0)
m	0.5	-6.45102	-0.0076562	-1.002476	**-6.45099**	**-0.0076560**	**-1.002474**
	1	-6.53071	-0.0481799	-1.002487	**-6.53067**	**-0.0481790**	**-1.002486**
	1.5	-6.62365	-0.1194525	-1.002588	**-6.62364**	**-0.1194522**	**-1.002582**
Rd	0.5	-6.44609	-0.0130798	-1.002478	**-6.44608**	**-0.0130791**	**-1.002476**
	1.5	-6.53071	-0.0481799	-1.002487	**-6.53067**	**-0.0481792**	**-1.002484**
	5	-6.67127	-0.0949682	-1.002634	**-6.67122**	**-0.0949680**	**-1.002630**
Q	0.5	-6.44608	-0.013082	-0.995255	**-6.44602**	**-0.013079**	**-0.995252**
	1	-6.44606	-0.013081	-0.994049	**-6.44601**	**-0.013075**	**-0.994042**
	1.5	-6.44604	-0.013079	-0.990444	**-6.44600**	**-0.013069**	**-0.990439**
B	0.2	-5.17273	-0.001953	-0.997932	**-5.17268**	**-0.001952**	**-0.997930**
	0.4	-5.15858	-0.001984	-0.997928	**-5.15855**	**-0.001980**	**-0.997922**
	0.6	-5.14578	-0.002093	-0.997925	**-5.14572**	**-0.002090**	**-0.997926**
ϕ	0.05	-6.44609	0.027971	-1.002445	**-6.44601**	**0.027969**	**-1.002446**
	0.1	-6.56401	0.092948	-1.002456	**-6.56399**	**0.092944**	**-1.002457**
	0.15	-6.6933	0.165833	-1.002567	**-6.69250**	**0.165830**	**-1.002566**
β	0.2	-6.44608	-0.013087	-0.995255	**-6.44606**	**-0.013086**	**-0.995259**
	0.4	-5.81921	-0.008275	-0.993134	**-5.81930**	**-0.008276**	**-0.993132**
	0.6	-5.22743	-0.003886	-0.991125	**-5.22742**	**-0.0038888**	**-0.991127**
A	1.05	-5.12163	-0.002099	-0.997919	**-5.12165**	**-0.002097**	**-0.997920**
	1.15	-5.12167	-0.002082	-1.000456	**-5.12169**	**-0.002080**	**-1.000455**
	1.2	-5.12176	-0.002081	-1.005377	**-5.12172**	**-0.002079**	**-1.005376**

Table 3b : In the absence of Eckert number(Ec=0) the results are in good agreement with those of ***Reddy et al*** [38]

Parameter		Ethylene Glycol-TiO2 nanofluid Sreenivasa Reddy et al[38]			Ethylene Glycol-TiO2 nanofluid Present values		
		τx(0)	τy(0)	Nu(0)	τx(0)	τy(0)	Nu(0)
m	0.5	-6.40185	-0.007319	-1.00102	**-6.40179**	**-0.007259**	**-1.00096**
	1	-6.48053	-0.047942	-1.00106	**-6.48047**	**-0.047882**	**-1.00100**
	1.5	-6.57389	-0.118815	-1.00117	**-6.57383**	**-0.118755**	**-1.00111**
Rd	0.5	-6.39665	-0.013527	-1.00102	**-6.39659**	**-0.013467**	**-1.00096**
	1.5	-6.48053	-0.047942	-1.00106	**-6.48047**	**-0.047882**	**-1.00100**
	5	-6.62173	-0.094449	-1.00112	**-6.62167**	**-0.094389**	**-1.00106**
Q	0.5	-6.39664	-0.0108298	-1.001327	**-6.39658**	**-0.0107698**	**-1.001267**
	1	-6.39544	-0.0107455	-0.997689	**-6.39538**	**-0.0106855**	**-0.997629**
	1.5	-6.39535	-0.0090196	-0.996191	**-6.39529**	**-0.0089596**	**-0.996131**
B	0.2	-5.12368	-0.0019567	-1.001556	**-5.12362**	**-0.0018967**	**-1.001496**
	0.4	-5.10816	-0.0019708	-0.999249	**-5.10810**	**-0.0019108**	**-0.999189**
	0.6	-5.09512	-0.0019849	-0.999242	**-5.09506**	**-0.0019249**	**-0.999182**
ϕ	0.05	-6.39665	0.0291706	-1.001026	**-6.39659**	**0.0292306**	**-1.000966**
	0.1	-6.49823	0.0933258	-1.001066	**-6.49817**	**0.0933858**	**-1.001006**
	0.15	-6.61669	0.1666359	-1.001125	**-6.61663**	**0.1666959**	**-1.001065**
β	0.2	-6.39664	-0.0125298	-1.001325	**-6.39658**	**-0.0124698**	**-1.001265**

Parameter		Ethylene Glycol-TiO2 nanofluid Sreenivasa Reddy et al[38]			Ethylene Glycol-TiO2 nanofluid Present values		
		τx(0)	τy(0)	Nu(0)	τx(0)	τy(0)	Nu(0)
	0.4	-5.76833	-0.0062137	-0.997351	**-5.76827**	**-0.0061537**	**-0.997291**
	0.6	-5.17641	-0.0037926	-0.996557	**-5.17635**	**-0.0037326**	**-0.996497**
A	1.05	-5.07139	-0.002091	-1.001555	**-5.07133**	**-0.002031**	**-1.001495**
	1.15	-5.07235	-0.001668	-1.001866	**-5.07229**	**-0.001608**	**-1.001806**
	1.2	-5.07321	-0.001068	-1.002317	**-5.07315**	**-0.001008**	**-1.002257**

5. DISCUSSION OF THE NUMERICAL REASULTS:

We make an investigation of the three dimensional squeezing convective flow, heat transfer flow of an electrically conducting Water based Tio2 nanofluid and Ethylene Glycol based Tio2 nanofluiud in a vertical channel in the presence of internal heat generating source/sink. In our numerical simulation the default values of the parameters are considered as : S=0.4, M^2=0.5,, Q=0.5.m=0.5, β=0.5,ϕ=0.05,Rd=0.5,B=0.2,Ec=0.05,A=1.05, Pr=0.71,.In order to analyse the effects of various pertinent parameters on velocity, temperature and concentration profiles, several graphs are plotted. The axial velocity is positive, transverse velocity and temperature are negative for all variations. We follow the convention that the non-dimensional temperature (θ)is positive/negative according as the actual temperature(T) is greater /lesser than the ambient temperature (T_0).

Figure.2a-2c are plotted for f′,g,θ profiles against η for different values of G by fixing other parameters. Thermal Grashof number signifies the relative magnitude of the thermal buoyancy force and the opposing frictional force (viscous hydrodynamic force) acting on the nanofluids. It can seen from the profiles that the actual temperature decrease with increase in Grashof number G while the axial velocity f ′ reduces in the region (0,0.5) and enhances in the region(0.5,1) and the transverse velocity g enhances in the entire flow region (0,1.0) with increase in G. This may be attributed to the fact that an increase in G reduces the thickness of the momentum boundary layer and increases the thickness of the thermal boundary layer.The values of the axial velocity in water based Tio2 nanofluid are greater than the values in Eg based Tio2 nanofluid in the flow region (0,0.5) while in the region(0,5,1,0) opposite effect is observed. The values of transverse velocity and actual temperature in Water based Tiuo2 nanofluid are relatively smaller than those in Eg based Tio2 nanofluid.

Fig.3a-3c depict the effect of magnetic field parameter(M^2) on f′,g ,θ.the parameter M is related directly to the applied magnetic field strength H0.Increasding magnetic field strength therefore elevates the Lorentz drag force which inhibits f'. It can be found from the profiles that the transverse velocity component g enhances with increase in M in the entire flow region(fig.3a&3b),while the axial velocity f ′ reduces in the right half (0,0.5) and enhances in the left half (0.5,1.0) of the channel(fig.3a). Effectively the application of transverse magnetic field to the electrically conducting fluid nanofluid generates a resistive type force, which acts against the motion of the nanofluid. The thickness of the thermal boundary layers enhance with increase in M which results in a fall in the actual temperature in the flow region(figs.3c).However the application of the magnetic field achieves excellent flow control in the regime and provides a simple but effective mechanism for regulating nanomaterial's processing operation. The values of the axial velocity in water based Tio2 nanofluid are greater than the values in Eg based Tio2 nanofluid in the flow region (0,0.5) while in the region(0,5,1,0) opposite effect is observed. The values of transverse velocity in Water based Tiuo2 nanofluid are relatively greater than those in Eg based Tio2 nanofluid. The actual temperature in Water based Tio2 nanofluid are smaller than those in Eg based Tio2 nanofluid in the flow region(0,1.0).

The influence of Hall parameter(m) on f′,g,θ can be observed from the figs.4a-4c.The Hall parameter features arising in both the dimensionless primary and secondary momentum equations(2.15&2.16).The axial velocity f ′ reduces in the right half (0,0.5) and enhances in the left half (0.5,1.0) of the channel while transverse velocity g upsurges, actual temperature reduces with increase in m. This is due to the fact thickness of the thermal boundary layer decrease with m. The values of the axial velocity in (0,0.5),transverse velocity in (0,1) in Water based Tio2 nanofluid are relatively greater than those in Eg based Tio2 nanofluid. The axial velocity in (0.5,1) and actual temperature in (0,1)in Water based Tio2 nanofluid are smaller than those in Eg based Tio2 nanofluid.

Fgs.5a-5c show the influence of thermal radiation(Rd) on f ′,g,θ .It can be seen from the profiles(figs.5a-5b)that there is a significant depreciation in the magnitude of the velocity component f ′ in (0,0.5) and enhancement in (0.5,1).The transverse velocity(g) enhances, actual temperature reduces in the presence of thermal radiation throughout the flow region. The radiation parameter is found to reduce the hydrodynamic boundary layers along x and y-directions .the presence of the thermal radiation is very significant on the variation of temperature. It is seen that the temperature decreases rapidly in the presence of thermal radiation parameter throughout the flow region. This may be attributed to the fact that as the Roseland radiative absorption parameter R*diminishes the corresponding heat flux diverges and thus falling the rate of radiative heat transfer to the fluid causing a fall in the temperature of the fluid. The thickness of the thermal boundary layer also decreases with increase in Rd(fig.5c). The values of the axial velocity in (0,0.5),transverse velocity in (0,1) in Water based Tio2 nanofluid are relatively greater than those in Eg based Tio2 nanofluid. The axial velocity in (0.5,1) and actual temperature in (0,1)in Water based Tio2 nanofluid are smaller than those in Eg based Tio2 nanofluid.

Figs.6a-6c demonstrate the variation of f',g and θ with viscosity parameter(B).An increase in viscosity parameter(B) reduces the axial velocity f' in the flow region (0,0.5) while the velocity f' in the region(0.5,1.0),the transverse velocity(g),actual temperature in the flow region(0.1) upsurge in the entire flow region. The values of the axial velocity in (0,0.5),the actual temperature in (0,1) in Water based Tio2 nanofluid are relatively greater than those in Eg based Tio2 nanofluid.The axial velocity in (0.5,1) and transverse velocity (g) in the region (0,1)in Water based Tio2 nanofluid are smaller than those in Eg based Tio2 nanofluid.

Figs.7a-7c show the variation of f',g and θ with Eckert number(Ec).From the profiles we find that the axial velocity (f') in the flow region(0,0.5),transverse velocity(g),actual temperature depreciate in the flow region(0,1) while the axial velocity (f ') enhances in the flow region(0.5,1.0) with higher values of Ec .This may be attributed to the fact that the thickness of the momentum and thermal boundary layers become thinner with increase in dissipative energy. The values of the axial velocity in (0,0.5),transverse velocity, the actual temperature in (0,1) in water based Tio2 nanofluid are relatively smaller than those in Eg based Tio2 nanofluid.The axial velocity in (0.5,1) in Water based Tio2 nanofluid are greater than those in Eg based Tio2 nanofluid.

Figs.8a-8c are plotted to illustrate the effect of heat source parameter (Q) on the flow variables. It can be seen from the profiles that the axial velocity(f') in the flow region(0,0.5) and transverse velocity(g) in the flow region(0,1) reduce, while axial velocity in the region(0.5,1),actual temperature in the flow region(0,1) enhances with increase in the strength of the heat generating source. This may be attributed to the fact that in the presence of heat generating source, energy is absorbed in the flow region(figs.8a-8c). The values of the axial velocity in (0,0.5),transverse velocity in (0,1) in water based Tio2 nanofluid are relatively greater than those in Eg based Tio_2 nanofluid. The axial velocity in (0.5,1) and actual temperature in (0,1)in water based Tio_2 nanofluid are smaller than those in Eg based Tio_2 nanofluid.

The effect of nanoparticle volume fraction (ϕ) on f',g,θ can be seen from the figs.9a-9c.As the volume fraction increases ,the thermal conductivity of the nano-fluid is elevated. Therefore thermal diffusion is associated in the regime. It can be found from the profiles that an increase in nanoparticle volume fraction leads to a reduction in the axial velocity in the flow region(0,0.5) ,transverse velocity(g) in the region(0,1) while f' in the region(0.5,1), actual temperature in the region(0,1) enhances with increase in ϕ.This may be attributed to the fact that the thickness of the momentum boundary layer reduces with increase in ϕ. Also the thickness of the thermal boundary layer increases with increase in ϕ which leads to a rise in temperature in the flow region(figs.9c). The values of the axial velocity in (0,0.5), transverse velocity in (0,1),actual temperature in (0,1) in Water based Tio2 nanofluid are relatively greater than those in Eg based Tio_2 nanofluid. The axial velocity in (0.5,1) in Water based Tio2 nanofluid are smaller than those in Eg based Tio_2 nanofluid.

Figs.10a-10c represent the effect of non-linear thermal radiation on axial velocity, transverse velocity and temperature.From the graphs we find that the axial velocity(f '), transverse velocity(g) and actual temperature experience a depreciation in the entire flow region with rising values of temperature difference ratio(A).Thus the non-linear ity in thermal radiation results in a decay in all flow variables in the boundary layer. The values of the axial velocity in (0,1.0) in water based Tio2 nanofluid are relatively greater than those in Eg based Tio2 nanofluid. The transverse velocity in (0,1) and actual temperature in (0,1)in Water based Tio2 nanofluid are lesser than those in Eg based Tio2 nanofluid.

Figs.11a-11c illustrate the effect of suction on the flow variables. It can be seen from the profiles that an increase in suction parameter(fw>0) enhances the all the velocity components in the entire flow region(11a&11b).From figs.11c we find that the actual temperature reduces with suction parameter(fw>0). The values of the axial velocity in (0,1.0) in water based Tio2 nanofluid are relatively smaller than those in Eg based Tio2 nanofluid. The transverse velocity in (0,1) and actual temperature in (0,1)in Water based Tio2 nanofluid are greater than those in Eg based Tio2 nanofluid.

Figs.12a-12c present the typical profiles namely f ′,g,θ respectively for different values of the squeezing parameter (β).From figs.12a-12c show that the magnitude of the axial velocity (f ′) and transverse velocity(g) are increasing function functions of squeezing parameter(β). This implies that squeezing effect on flow field is accumulated by it An increase in β results in a depreciation in the temperature (figs.12c).This is due to the fact that a rise in squeezing parameter(β) values leads to a decrease in the thickness of the thermal boundary layer. The values of the axial velocity ,actual temperature in (0,1.0) in water based Tio2 nanofluid are relatively smaller than those in Eg based Tio2 nanofluid. The transverse velocity in (0,1) in water based Tio2 nanofluid are greater than those in Eg based Tio2 nanofluid.

The effect of Prandtl number(Pr) on f ′,g,θ can be seen from figs.13a-13c.Prndtl refers to the relative contribution of momentum diffusion to thermal diffusion in the boundary layer regime. Futhermore, an increase in Prandtl number results in a decrease in the actual temperature distribution in the thermal boundary layer. The physical reason is that smaller values of Prandtl number are associated with greater thermal conductivity, and therefore heat is able to diffuse away from the heated surface more rapidly than at higher values of Prandtl number i.e the energy diffusion rate is greater than the momentum diffusion rate for Pr<1 where as the converse is evident for Pr>1.For Pr=1 both the energy and momentum diffusion rates are the same. Effectively the rate of heat transfer is reduced and an increase in Pr induces a reduction in the thickness of the thermal boundary layer. From the profiles we find that all the axial velocity(f'),transverse velocity(g),actual temperature in (0,1) experience a depreciation in the region while in the region(0.5,1,0) the axial velocity enhances, with increase in Pr. Also lesser the thermal diffusivity smaller the thickness of the thermal boundary layer in the entire flow region(figs.13c). The values of the axial velocity in (0,0.5) ,the actual temperature in (0,1) in water based Tio2 nanofluid are relatively smaller than those in Eg based Tio2 nanofluid. The axial velocity in (0.5,1), transverse velocity in (0,1) in water based Tio2 nanofluid are greater than those in Eg based Tio2 nanofluid.

The Skin friction components τx,τy,Nusselt number on the walls ($(\eta = 0,1)$ are exhibited in tables.2 for different parametric variations. Increase in Grashof number enhances (τx) at left wall and reduces at the right wall . (τy) reduces at η=0 and enhances at η=1.Higher Lorentz force smaller (τx) and larger (τy) at both walls. (τx) and (τy) grow at η=0&1with increase in Hall parameter(m)/ radiation parameter(Rd)/nanoparticle volume fraction(ϕ)/ suction parameter(fw). (τx) and (τy) decay with higher values of Ec/Q/β at left wall(η=0). (τx) decays at η=0 and grows at η=1 with higher values of viscosity parameter(B) while opposite effect is noticed in (τy) at η=0 and 1. At right wall(η=1), (τx) enhances with Ec/B and reduces with Q/Pr and (τy)enhances with Q/Pr,decays with E/B.Increase in temperature difference ratio(A) reduces (τx) at left wall and enhances at right wall while opposite effect is observed in (τy) at η=0 and 1 in both types of nanofluids. For an increase in M/m/Rd/Ec/Q/B/fw/A, the skin friction components at left wall(η=0)in water based Tio2 nanofluids are relatively greater than those in Eg based Tio2 nanofluid while reversed effect is noticed with rising values of G/ϕ/Pr.At the right wall(η=1)for an increase in M/m/Rd/Ec/Q/B/β/A/Pr,the values of skin friction components in water based Tio2 nanofluid are lesser than those in Eg based Tio2 nanofluid.For rising values of ϕ/fw, values of (τx) and (τy) in water based Tio2 nanofluid are grater than those in Eg based Tio2 nanofluid.

The rate of heat transfer(Nu) enhances with increase in G/M/m/Rd /ϕ/A and reduces with increase in B/fw/Pr at left wall(η=0) in both types of nanofluids.Nu reduces with Q/β and enhances with Ec in Water based Tio2 nanofluid while in Eg based Tio2 nanofluid, it reduces with Ec at η=0. At the right wall(η=1) Nu grows with higher values of G/Q/β/fw/Pr and decays with M/m/Rd/Ec/B/ϕ/A,in both types of nanofluids. Fr an increase in G/Ec/Q/ S(β)/A/Pr ,the values of Nusselt number in water based Tio2 nanofluid are relatively smaller than those in Eg based Tio2 nanofluid while opposite effect is observed win Nu with variations in M/m/Rd/ϕ/fw.At the right wall(η=1)for variations in G/MQ/B/β/fw/A/Pr,the values of Nusselt number in water based Tio2 nanofluid are relatively greater than those in Eg based Tio2 nanofluid while for variations in m/ϕ,opposite effect is noticed in Nu in water /Eg based Tio2 nanofluids.

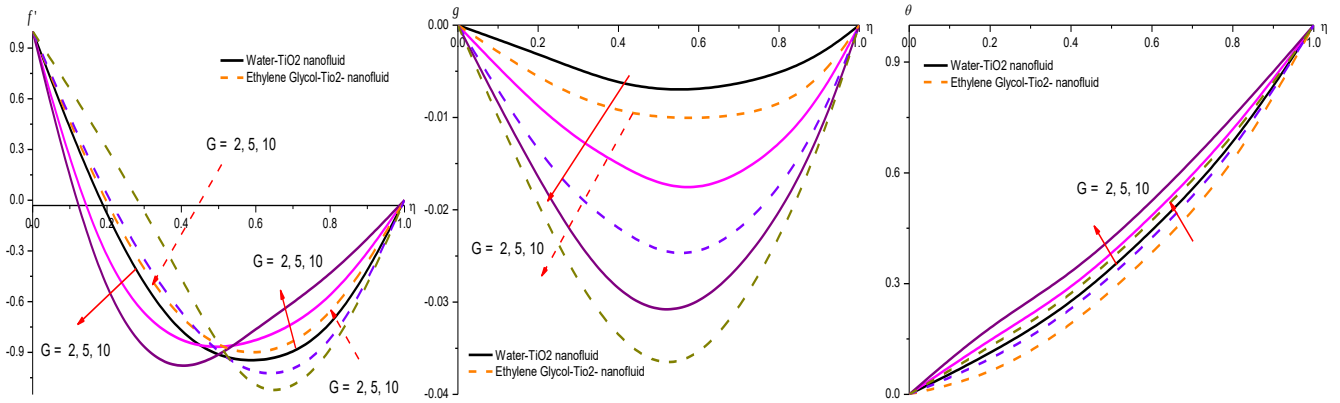

Fig.2 : Variation of [a] Primary velocity(f'), [b]Secondary velocity (g),
[c] Temperature(θ),with G
M=0.5, m=0.5, Rd=0.5, B=0.2, Ec=0.1, Q=0.5, ϕ=0.05, A=0.5, fw=0.1, β=0.2, Pr=0.71,

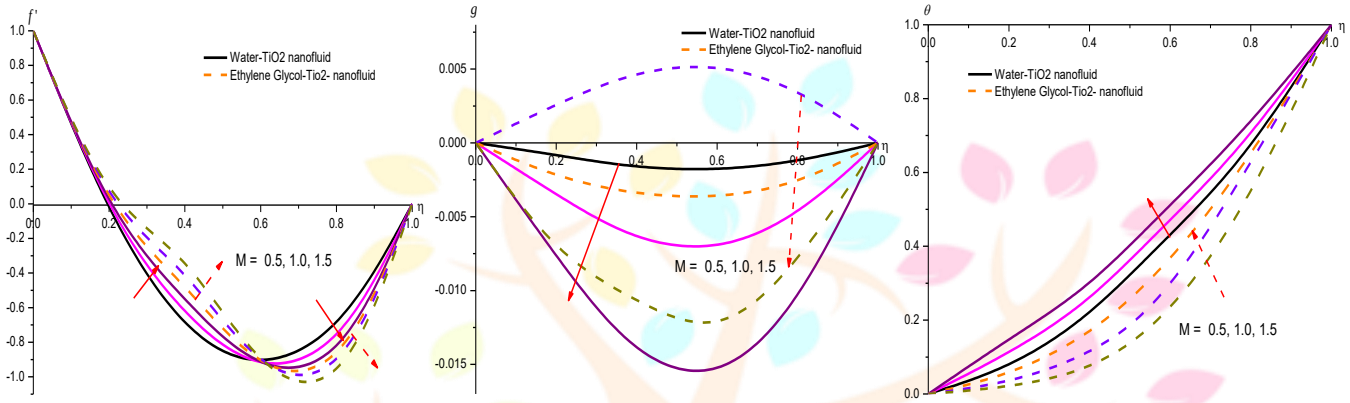

Fig.3 : Variation of [a] Primary velocity(f'), [b]Secondary velocity (g),
[c] Temperature(θ) with M
G=2, m=0.5, Rd=0.5, B=0.2, Ec=0.1, Q=0.5, ϕ=0.05, A=0.5, fw=0.1, β=0.2

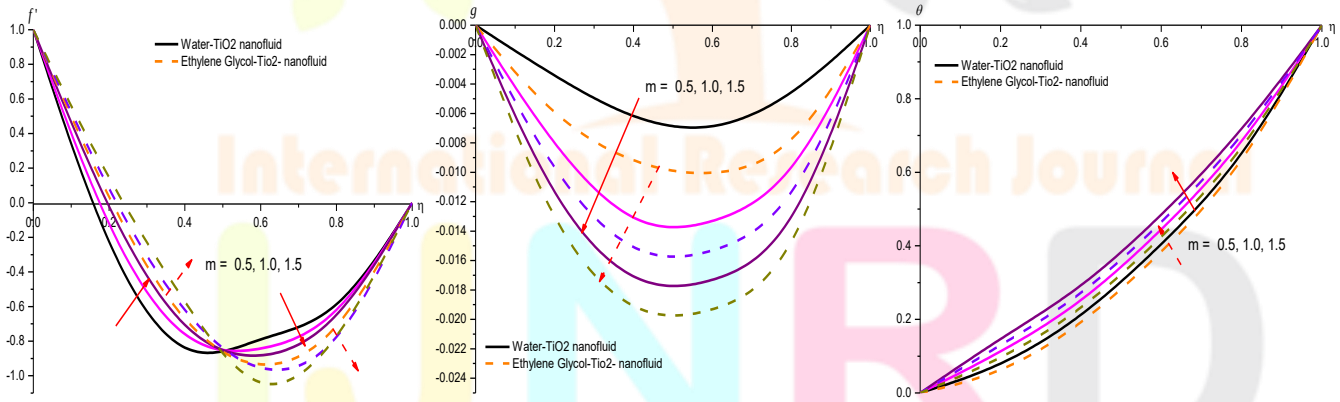

Fig.4 : Variation of [a] Primary velocity(f'), [b]Secondary velocity (g),
[c] Temperature(θ) with m
G=2, M=0.5, Rd=0.5, B=0.2, Ec=0.1, Q=0.5, ϕ=0.05, A=0.5, fw=0.1, β=0.2

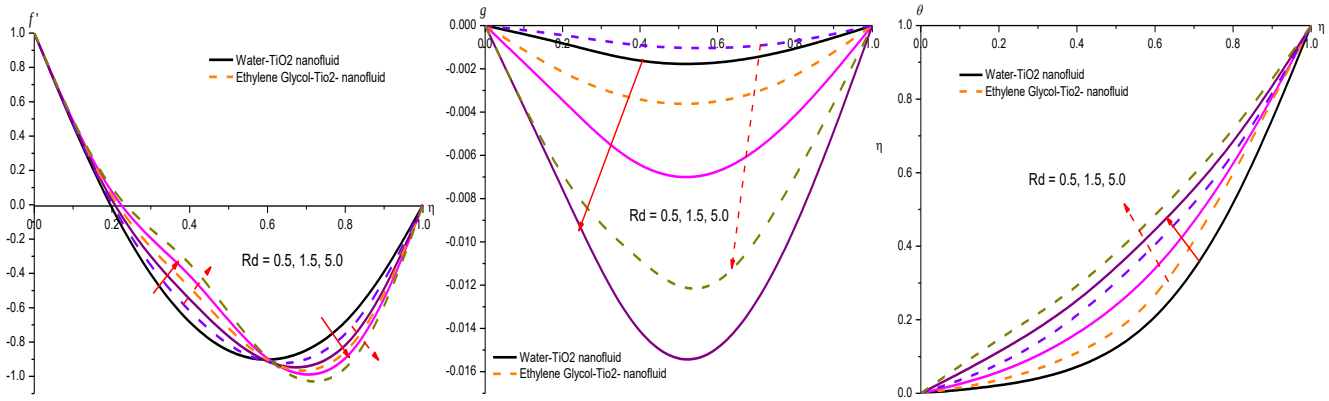

Fig.5 : Variation of [a] Primary velocity(f'), [b]Secondary velocity (g),

[c] Temperaturewith Rd

G=2, M=0.5, *m*=0.5, B=0.2, Ec=0.1, Q=0.5, ϕ=0.05, A=0.5, fw=0.1, β=0.2, Pr=0.71,

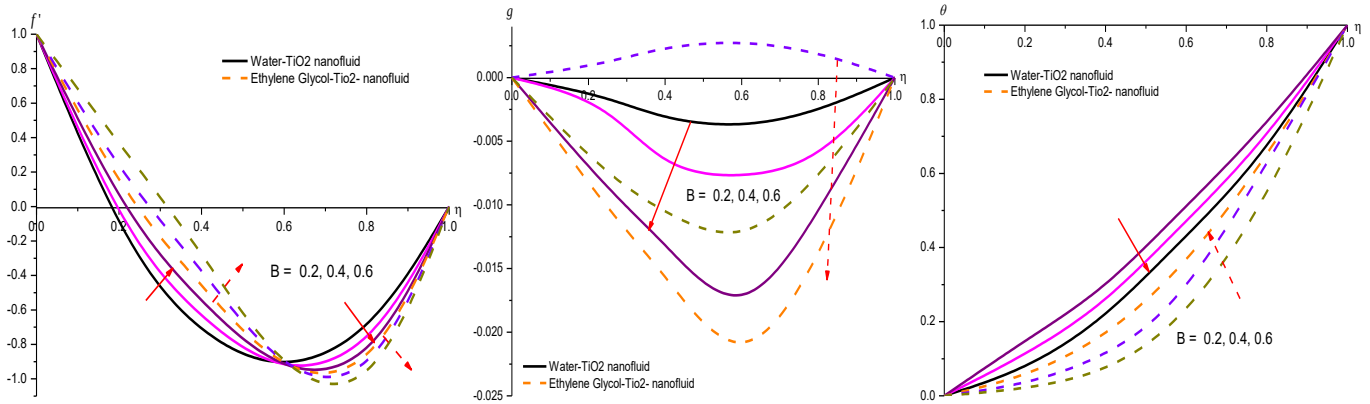

Fig.6 : Variation of [a] Primary velocity(*f '*), [b]Secondary velocity (*g*),
[c] Temperature(θ),with B

G=2, M=0.5, *m*=0.5, Rd=0.5, Ec=0.1, Q=0.5, ϕ=0.05, A=0.5, fw=0.1, β=0.2, Pr=0.71,

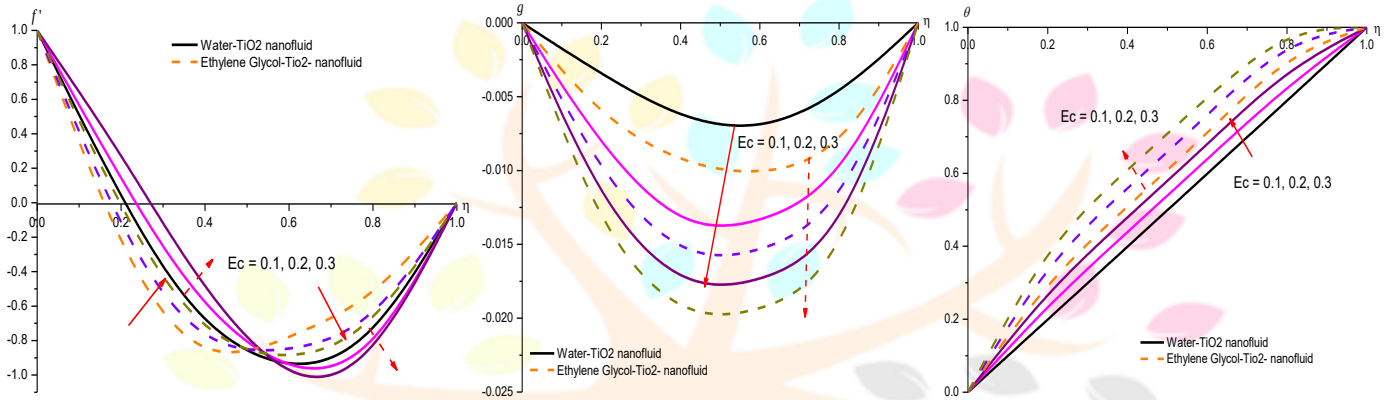

Fig.7 : Variation of [a] Primary velocity(*f '*),[b] Secondary velocity (*g*),
[c] Temperature(θ),with Ec

G=2, M=0.5, *m*=0.5, Rd=0.5, B=0.2, Q=0.5, ϕ=0.05, A=0.5, fw=0.1, β=0.2, Pr=0.71

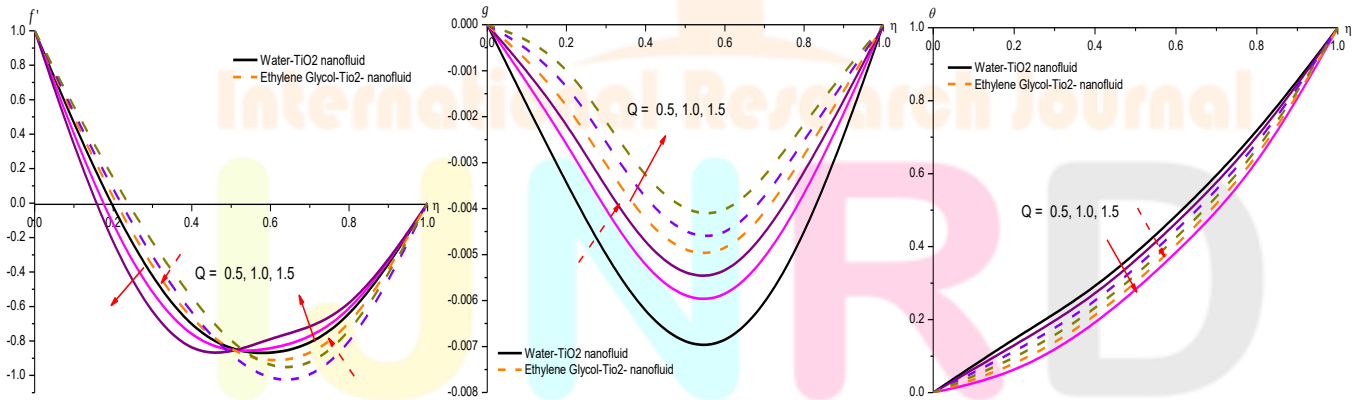

Fig.8 : Variation of [a] Primary velocity(*f '*), [b]Secondary velocity (*g*),
[c] Temperature(θ),with Q

G=2, M=0.5, *m*=0.5, Rd=0.5, B=0.2, Ec=0.1, ϕ=0.05, A=0.5, fw=0.1, β=0.2, Pr=0.71

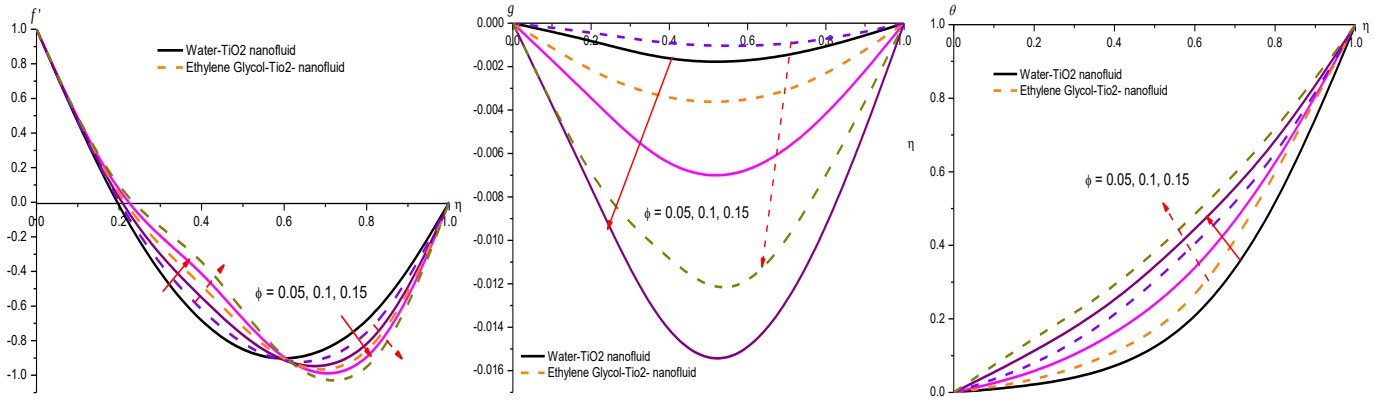

Fig.9 : Variation of [a] Primary velocity(f'),[b] Secondary velocity (g),
[c] Temperature(θ),with ϕ
G=2, M=0.5, m=0.5, Rd=0.5, B=0.2, Ec=0.1, Q=0.5, A=0.5, fw=0.1, β=0.2, Pr=0.71

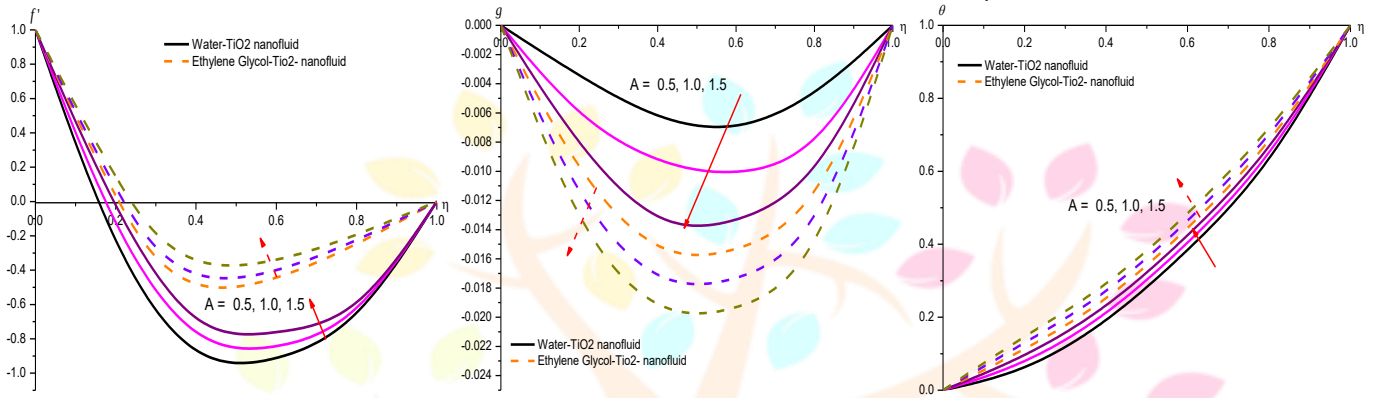

Fig.10 : Variation of [a] Primary velocity(f'),[b] Secondary velocity (g),
[c] Temperature(θ),with A
G=2, M=0.5, m=0.5, Rd=0.5, B=0.2, Ec=0.1, Q=0.5, ϕ=0.05, fw=0.1, β=0.2, Pr=0.71

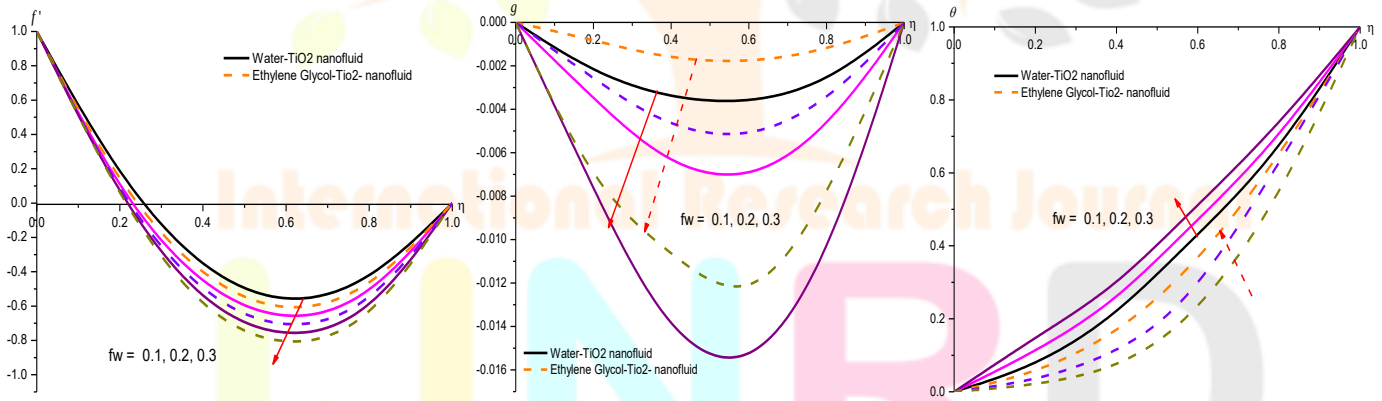

Fig.11 : Variation of [a] Primary velocity(f'),[b] Secondary velocity (g),
[c] Temperature(θ),with fw
G=2, M=0.5, m=0.5, Rd=0.5, B=0.2, Ec=0.1, Q=0.5, ϕ=0.05, A=0.5, β=0.2, Pr=0.71

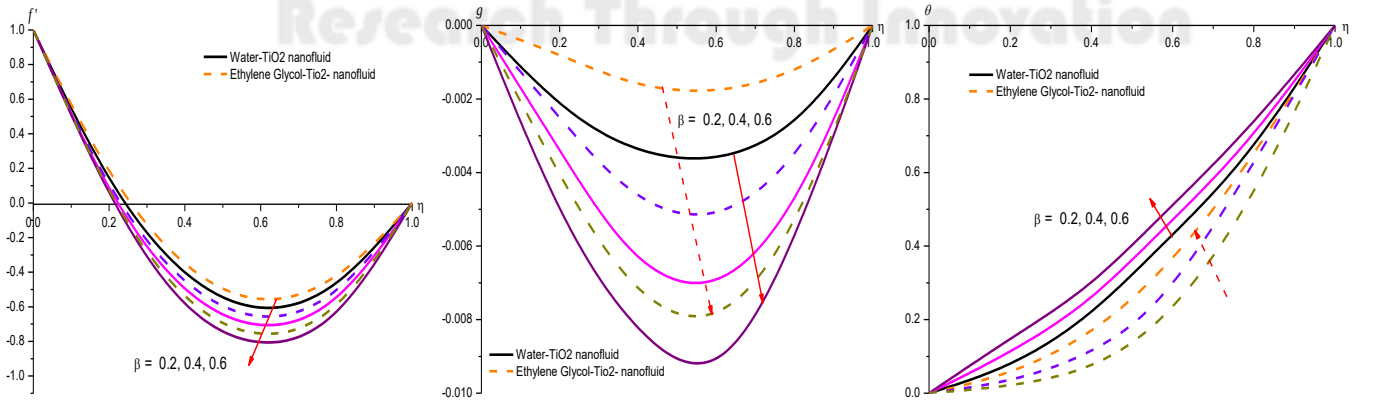

Fig.12 : Variation of [a] Primary velocity(f'), [b] Secondary velocity (g),
[c] Temperature(θ),with β
G=2, M=0.5, m=0.5, Rd=0.5, B=0.2, Ec=0.1, Q=0.5, ϕ=0.05, A=0.5, fw=0.1, Pr=0.71

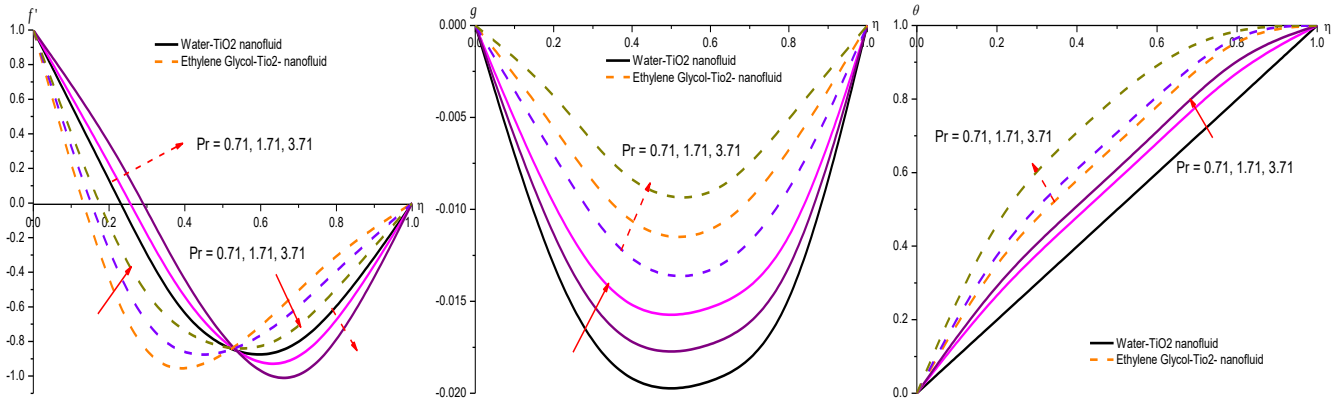

Fig.13 : Variation of [a] Primary velocity(f'), Secondary velocity (g),
[c] Temperaturewith Pr
G=2, M=0.5, m=0.5, Rd=0.5, B=0.2, Ec=0.1, Q=0.5, ϕ=0.05, A=0.5, fw=0.1, β=0.2

Table 3a :

Parameter		Water-TiO2 nanofluid			Ethylene Glycol-TiO2 nanofluid		
		τx(0)	τy(0)	Nu(0)	τx(0)	τy(0)	Nu(0)
G	2	-6.44609	4.9064523	0.027971	-6.39665	4.963214	0.02916
	4	-6.71814	4.7002634	0.105404	-6.61848	4.812793	0.10663
	6	-7.04123	4.5069145	0.217266	-6.89402	4.672944	0.21991
M	0.5	-6.41078	-0.0033373	-1.002373	-6.37428	-0.003357	-1.00101
	1	-6.38951	-0.0130473	-1.002474	-6.33873	-0.009728	-1.00102
	1.5	-6.35378	-0.0282596	-1.002535	-6.30275	-0.028121	-1.00103
m	0.5	-6.45102	-0.0076562	-1.002476	-6.40185	-0.007319	-1.00102
	1	-6.53071	-0.0481799	-1.002487	-6.48053	-0.047942	-1.00106
	1.5	-6.62365	-0.1194525	-1.002588	-6.57389	-0.118815	-1.00117
Rd	0.5	-6.44609	-0.0130798	-1.002478	-6.39665	-0.013527	-1.00102
	1.5	-6.53071	-0.0481799	-1.002487	-6.48053	-0.047942	-1.00106
	5	-6.67127	-0.0949682	-1.002634	-6.62173	-0.094449	-1.00112
Ec	0.1	-5.12163	-0.0020824	-0.997915	-5.07139	-0.0019897	-1.00155
	0.2	-5.12162	-0.0020822	-0.998076	-5.07035	-0.0016683	-0.999301
	0.3	-5.1216	-0.0020819	-0.998277	-5.07024	-0.0012168	-0.998362
Q	0.5	-6.44608	-0.013082	-0.995255	-6.39664	-0.0108298	-1.001327
	1	-6.44606	-0.013081	-0.994049	-6.39544	-0.0107455	-0.997689
	1.5	-6.44604	-0.013079	-0.990444	-6.39535	-0.0090196	-0.996191
B	0.2	-5.17273	-0.001953	-0.997932	-5.12368	-0.0019567	-1.001556
	0.4	-5.15858	-0.001984	-0.997928	-5.10816	-0.0019708	-0.999249
	0.6	-5.14578	-0.002093	-0.997925	-5.09512	-0.0019849	-0.999242
ϕ	0.05	-6.44609	0.027971	-1.002445	-6.39665	0.0291706	-1.001026
	0.1	-6.56401	0.092948	-1.002456	-6.49823	0.0933258	-1.001066
	0.15	-6.6933	0.165833	-1.002567	-6.61669	0.1666359	-1.001125
β	0.2	-6.44608	-0.013087	-0.995255	-6.39664	-0.0125298	-1.001325
	0.4	-5.81921	-0.008275	-0.993134	-5.76833	-0.0062137	-0.997351
	0.6	-5.22743	-0.003886	-0.991125	-5.17641	-0.0037926	-0.996557
fw	0.1	-5.12163	-0.002182	-0.997919	-5.07139	-0.0020917	-1.001554
	0.2	-6.44608	-0.013082	-0.995255	-6.39543	-0.0097456	-0.998189
	0.3	-7.72907	-0.024927	-0.992628	-7.67902	-0.0248692	-0.997155
A	1.05	-5.12163	-0.002099	-0.997919	-5.07139	-0.002091	-1.001555
	1.15	-5.12167	-0.002082	-1.000456	-5.07235	-0.001668	-1.001866
	1.2	-5.12176	-0.002081	-1.005377	-5.07321	-0.001068	-1.002317
Pr	0.71	-6.44608	-0.013082	-0.995235	-6.39664	-0.013598	-1.001324
	1.71	-6.44607	-0.013083	-0.991516	-6.39545	-0.013745	-0.996694
	6.2	-6.44606	-0.013086	-0.981059	-6.39537	-0.014019	-0.992498

Table 3b :

Parameter		Water-Tio2 nanofluid			Ethylene Glycol-Tio2 nanofluid		
		τx(+1)	τy(+1)	Nu(+1)	τx(+1)	τy(+1)	Nu(+1)
G	2	4.90645	-0.013079	-1.002484	4.96321	-0.013529	-1.00102
	4	4.70026	-0.049164	-1.002494	4.81279	-0.048664	-1.00106
	6	4.50691	-0.099269	-1.002653	4.67294	-0.097601	-1.00112
M	0.5	4.90351	0.0070826	-0.996341	4.96174	0.0071577	-0.998465
	1	4.90204	0.0280166	-0.996317	4.95956	0.0205467	-0.998456
	1.5	4.89956	0.0618998	-0.996278	4.95723	0.0620935	-0.998439
m	0.5	4.90633	0.0164061	-0.996314	4.96352	0.0171078	-0.998452
	1	4.91268	0.1066452	-0.996226	4.96932	0.1069786	-0.998415
	1.5	4.92287	0.2742553	-0.996117	4.97899	0.2751285	-0.998372
Rd	0.5	4.90645	0.0279714	-0.996316	4.96321	0.0291706	-0.998455
	1.5	4.91268	0.1066455	-0.996227	4.96932	0.1069784	-0.998415
	5	4.92576	0.2226156	-0.996061	4.98164	0.2233334	-0.998349
Ec	0.1	3.23579	0.0165416	-0.999549	3.29261	0.0172881	-0.997756
	0.2	3.23589	0.016541	-0.999429	3.29267	0.0121369	-0.997086
	0.3	3.23599	0.0165406	-0.999314	3.29269	0.0166273	-0.996638
Q	0.5	4.90597	0.0279703	-1.000665	4.96328	0.0291706	-0.997851
	1	4.9059	0.0279706	-1.003087	4.96309	0.0305168	-1.001176
	1.5	4.90577	0.0279709	-1.010345	4.96296	0.0310562	-1.004189
B	0.2	3.23579	0.0165416	-0.999549	3.29261	0.0172881	-0.997756
	0.4	3.23581	0.0165386	-0.998176	3.29267	0.0170366	-0.997342
	0.6	3.23582	0.0165306	-0.997478	3.29269	0.0166273	-0.9969227
ϕ	0.05	-0.01379	-1.002434	-0.996316	-0.01352	-1.001024	-0.998455
	0.1	-0.04423	-1.002455	-0.996242	-0.04115	-1.001065	-0.998413
	0.15	-0.06846	-1.002559	-0.996112	-0.06925	-1.001126	-0.998345
S	0.2	4.90597	0.0279703	-1.000663	4.96326	0.029176	-0.997851
	0.4	4.22753	0.0229136	-1.005043	4.28489	0.020804	-1.001978
	0.6	3.58728	0.0182611	-1.009214	3.64493	0.018346	-1.003548
fw	0.1	3.23579	0.0165416	-0.999549	3.29261	0.0172881	-0.997756
	0.2	4.90597	0.0279703	-1.000667	4.96309	0.0205161	-1.000178
	0.3	6.62248	0.0395396	-1.001745	6.68005	0.0396261	-1.000689
A	1.05	3.23579	0.0165416	-0.999549	3.29261	0.0172881	-0.997756
	1.15	3.23582	0.0165417	-0.996235	3.29267	0.0181366	-0.996366
	1.2	3.23588	0.0165418	-0.989265	3.29278	0.0196274	-0.995473
Pr	0.71	4.90597	0.0279703	-1.000696	4.96323	0.0291706	-0.997853
	1.71	4.90596	0.0279756	-1.004397	4.96314	0.0305166	-1.001688
	6.2	4.90592	0.0279894	-1.014874	4.96309	0.032 0558	-1.005919

5. CONCLUSIONS:

1) An increase in G reduces the axial velocity, actual concentration, enhances the transverse velocity. The skin friction component (τx), Nusselt number increase and (τz) reduces at η=0 and at η=1, τx, Nu reduce, τz enhances with G.
2) Higher the Lorentz force smaller the axial velocity ,actual concentration, and larger the transverse velocity. The skin friction (τx)reduces, τz,Nu enhances at η=0.while at η=1, τx, Nu decay, τz grows with increase in M.
3) An increase in Hall parameter(m) reduces the axial velocity, actual temperature while the transverse velocity enhances. The skin friction components, Nu grows at η=0 and decays at η=1,with increase in m .
4) An increase in nanoparticle volume concentration (ϕ) enhances the velocities and reduces the actual temperature .The skin friction components grow at both the walls while Nu enhances at η=0,decays at η=1with increase in ϕ.
5) Higher thermal radiation(Rd) smaller the axial velocity, actual temperature and larger the transverse velocity. The skin friction components grow at both the walls while Nu enhances at η=0,decays at η=1with increase in ϕRd.
6) An increase in the squeezing parameter(β) enhances the velocities and reduces the actual temperature .An increase in β reduces the skin friction components at both the walls while Nu decays at η=0 and grows at η=1.
7) An increase in heat source parameter(Q) reduces the velocities and enhances the actual, temperature and.τx decay at both walls. ,τy decays at left all and grows at right wall. Nu reduces at η=0 and grows at η=1 in water based Tio2 nanofluid while Nu groes at both walls in both types of nanofluids.
8) Increase in temperature difference ratio(A) depreciates the velocities and actual; temperature. τx, grows at η=0&1in both types of nanofluids. ,τy decreases at left wall and enhances at right wall in both types of nanofluids. Nu enhances at η=0 and reduces at η=1 in both types of nanofluids with rising values of A.
9) Higher the dissipative energy smaller the velocities, and actual temperature. τx reduces at left wall and enhances at right wall in both types of nanofluis. τy decays at η=0&1 in both types of nanofluids. Nu enhances at η=0&1 in water based Tio2 nanofluid while in Eg based Tio2 nanofluid, Nu decays with Ec in both types of nanofluids.

10) The velocities enhances and actual temperature reduces with fw>0. τx, τy grow at η=0&1 in both types of nanofluids, reduces at left wall and enhances at right wall with fw. Decays on the walls with rise in fw.

6. REFERENCES

[1]. Ali ME. The effect of variable viscosity on mixed convection heat transfer along a vertical moving surface. Int J Thermal Sci (2006):45:60-9.

[2]. Brewester, M.Q : Thermal radiative transfer and properties. John Wiley & Sons. Inc. New York (1992).

[3]. Buongiorno J. : Convective transport in nanofluids, ASME J. Heat Transfer, V.128, pp. 240–250(2006).

[4]. Chen,H,Witharana,S,Jin,Y,Kim C,Ding Y:Predicting thermal conductivity of liquid suspensions of nanoparticles(nanofluids)based on rheology,Particuology,Vol.y,pp.151-157(2009)

[5]. Choi S.U.S., Siginer D.A., Wang H.P. : Enhancing Thermal Conductivity of Fluids with Nanoparticles, Developments and Applications of Non-Newtonian Flows, The American Society of Mechanical Engineers, New York, FED-vol. 231/MDvol. 66, pp. 99–105 (1995).

[6]. Das K. : Flow and heat transfer characteristics of nanofluids in a rotating frame, Alexandria Eng. J., 53 (3), pp.757–766(2014).

[7]. Devasena Y: effect of non-linear thermal radiation, activation energy on hydromagnetic convective heat and mass transfer flow of nanofluid in vertical channel with Brownian motion and thermophoresis in the presence of irregular heat sources, *World Journal of Engineering Research and Technology* (JERT) *wjert, (2023), Vol. 9, Issue 2, XX-XX*, ISSN 2454-695X, SJIF Impact Factor: 5.924, www.wjert.org

[8]. Devi SPA, Prakash M. Temperature-dependent viscosity and thermal conductivity effects on hydromagnetic flow over a slendering stretching sheet. J of Nig Math Soc. (2015);34:318-330.

[9]. Domairry, G. and Aziz, A: Approximate analysis of MHD squeeze flow between two parallel disks with suction or injection by homotopy perturbation method", *Mathametical Problems in Engineering* , Vol. 2009. doi: 10.1155/2009/603916(2009)

[10]. Eastman J.A., Choi S.U.S., Li S., Yu W., Thompson L.J. : Anomalously increased effective thermal conductivity ofethylene glycol-based nanofluids containing copper nanoparticles, Appl. Phys. Lett. V.78, pp. 718–720 (2001).

[11]. Freidoonimehr N., Rostami B, Rashidi M.M., Momoniat E. : Analytical modelling of three-dimensional squeezing nanofluid flow in a rotating channel on a lower stretching porous wall, Math. Probl. Eng., 2014,14, 692728 (2014).

[12]. Gireesha B.J., Mahanthesh B., Gorla R.S.R. : Suspended particle effect on nanofluid boundary layer flow past a stretching surface, J. Nanofluids, V.3 (3), pp. 267–277 (2014).

[13]. Hamad M.A.A., Pop I. : Unsteady MHD free convection flow past a vertical permeable flat plate in a rotating frame of reference with constant heat source in a nanofluid, Heat Mass Transfer, V.47, pp.1517–1524 (2011).

[14]. Hamza, E.A. (1999), Suction and injection effects on a similar flow between parallel plates,*Journal of Physics D: Applied Physics* , Vol. 32 No. 6, pp. 656-663.

[15]. Hamza, E.A. and Macdonald, D.A. (1981), A fluid film squeezed between two parallel plane surfaces, *Journal of Fluid Mechanics* , Vol. 109, pp. 147-160.

[16]. Hayat, T. , Qayyum, A. and Alsaedi, A. (2015), "Three-dimensional mixed convection squeezing flow", *Applied Mathematics and Mechanics – English Edition.* , Vol. 36 No. 1, pp. 47-60.

[17]. Issac LA, Anselm OO. Effects of variable viscosity, dufour, soret and thermal conductivity on free convective heat and mass transfer of non-Darcian flow past porous at surface. Amer J of Comp Math (2014);4:357-365.

[18]. Kuznetsov A.V., Nield D.A. : Natural convective boundary layer flow of a nanofluid past a vertical plate, Int. J. Therm. Sci. V.49, pp.243–247, (2010).

[19]. Mahanthesh B, Gorla R S R, Gireesha B J : "Mixed convection squeezing three-dimensional flow in a rotating channel filled with nanofluid", *International Journal of Numerical Methods for Heat & Fluid flow*, V.26, Issue 5, pp.25-32(2016)

[20]. Makinde O.D., Mabood F, Khan W.A., Tshehla M.S. : MHD flow of a variable viscosity nanofluid over a radially stretching convective surface with radiative heat, Journal of Molecular Liquids, 219, (2016), pp.624-630, www.elsevier.com/ locate/molliq, http://dx.doi.org/10.1016 /j.molliq. 2016.03.078

[21]. Mebarek–Oudina F:Transient thermique convectif des nanofluides dans un espace annulaire entre deux culindres verticaux avec une source de chaleur., J.In. Thermique, Monstir (2017)

[22]. Mebarek –Oudina,:Convective heat transfer of Titania nanofluids of different base fluids in cylindrical annulus with discrete heat source.,Heat transfer-Asian Res.Vol.48,pp.135-147(2019)

[23]. Munawar, S. , Mehmood, A. and Ali, A. (2012), Three-dimensional squeezing flow in a rotating channel of lower stretching porous wall, *Computers and Mathematics with Applications* , Vol. 64 No. 6, pp. 1575-1586.

[24]. Mustafa, M. , Hayat, T. and Obaidat, S. (2012), On heat and mass transfer in the unsteady squeezing flow between parallel plates, *Meccanica* , Vol. 47 No. 7, pp. 1581-1589.

[25]. Nagasasikala M : Effect of activation energy on convective heat and mass transfer flow of dissipative nanofluid in vertical channel with Brownian motion and thermophoresis in the presence of irregular heat sources, *World Journal of Engineering Research and Technology* (JERT) *wjert, 2023, Vol. 9, Issue 2, XX-XX*, ISSN 2454-695X, SJIF Impact Factor: 5.924, www.wjert.org

[26]. Oztop. H. F and Abu-Nada. E (2008): Numerical study of natural convection in partially heated rectangular enclosures filled with nanofluids.,Int.J.Heat and Fluid Flow.,V.29,pp.1326-1336.

[27]. Pak BC,Cho YI:Hydrodynamic and heat transfer study of dispersed fluids with submicron metallic oxide particles,Exp.Heat Transf.,Vol.11,pp.151-170(1998)

[28]. Reddy PS,Chamkha AJ:Soret and Dufour effects on MHD convective flow of Al2o3-water and Tio2-water nanofluids past a strtching sheet in porous media with heat generating /absorption .Adv.Power Technol.Vol.27(4),pp.1207-1218(2016)

[29]. Satya Narayana K and Ramakrishna G N (2023) Effect of variable viscosity, activation energy and irregular heat sources on convective heat and mass transfer flow of nanofluid in a channel with brownian motion and thermophoresis, *World Journal of Engineering Research and Technology* (WJERT), *2023, Vol. 9, Issue 2, XX-XX*, ISSN 2454-695X, SJIF Impact Factor: 5.924, www.wjert.org

[30]. Sheikholeslami M., Ganji D.D. : Magnetohydrodynamic flow in a permeable channel filled with nanofluid, Sci. Iran, V.21 (1) , pp. 203–212 (2014).

[31]. Sheikholeslami M., Ganji D.D. : Unsteady nanofluid flow and heat transfer in presence of magnetic field considering thermal radiation, J. Braz. Soc. Mech. Sci. Eng. http://dx.doi.org/10. 1007/s40430-014-0228-x.
[32]. Sreenivasulu P, Poornima T, Bhaskar R. Variable thermal conductivity influence on hydromagnetic flow past a stretching cylinder in a thermally strati_ed medium with heat source/sink. Fron in Heat and Mass Trans.(2017);9(20):1-7
[33]. Stefan, M.J:Versuch U ber die scheinbare adhesion Sitzungsberichte der Akademie der Wissenschaften in Wien, *Mathematik-Naturwissen* , Vol. 69, pp. 713-721(1874).
[34]. Turkyilmazoglu M. : Exact analytical solutions for heat and mass transfer of MHD slip flow in nanofluids, Chem. Eng. Sci., V.84, pp.182–187 (2014).
[35]. Turkyilmazoglu M., Pop I. : Heat and mass transfer of unsteady natural convection flow of some nanofluids past a vertical infinite flat plate with radiation effect, Int. J. Heat Mass Transfer, V.59, pp.167–171(2013).
[36]. Vajravelu K, Prasad KV, Chiu-on N. Unsteady convective boundary layer flow of a viscous fluid at a vertical surface with variable fluid properties. Nonl Analy: Real World Appl. (2013);14:455-464.
[37]. Wang X, Xu X, Choi S.U.S. : Thermal conductivity of nanoparticle fluid mixture, J. Thermophys. Heat Transfer, V.13, pp.474–480(1999).
[38]. Sreenivasa Reddy B and Tulasilakshmi Devi B : Three-dimentional squeezing flow of Titania nanofluid in different base fluids with heat sources, Journal of Engineering, Computing & Architecture, Vol 13, Issue 12, December – 2023, pp.58-69, ISSN NO:1934-7197, DOI:17.0002.JECA.2023.V13I12.200786.22010
[39]. Einstein, A. (1906) Eineneue Bestinunung der Molekul dimension. Annals of Physics, 19, 286-306.
[40]. Gebhar, B. (1962) Effects of Viscous Dissipation in Natural Convection. Journal of Fluid Mechanics , 14, 225-232. https://doi.org/10.1017/S0022112062001196
[41]. Kishore, P.M., Rajesh, V. and Verma, S.V.K. (2010) Effects of Heat Transfer and Viscous Dissipation on MHD Free Convection Flow past an Exponentially Accelerated Vertical Plate with Variable Temperature. Journal of Naval Architecture and Marine Engineering, 7, 101-110.
[42]. Sakiadis, B.C. (1961) Boundary-Layer Behavior on Continuous Solid Surfaces, AIChE Journal, 7, 26-28.
[43]. Jewel Rana B. M., Roy Raju, Ershad Ali Lasker, Ahmmed S. F.:Radiation Absorption and Variable Electrical Conductivity Effect on High Speed MHD Free Convective Flow past an Exponential, Accelerated Inclined Plate, World Journal of Mechanics, 2017, 7, 211-241, https://doi.org/10.4236/wjm.2017.78019, http://www.scirp.org/journal/wjm, ISSN Online: 2160-0503